

# Transformers à Grande Vitesse

Massively parallel real-time predictions of train delay propagation

Farid Arthaud  
farto@csail.mit.edu  
Ecole Normale Supérieure  
Paris, France  
SNCF Réseau  
Saint-Denis, France

Guillaume Lecoeur  
Alban Pierre  
ext.guillaume.lecoeur@reseau.sncf.fr  
ext.alban.pierre@reseau.sncf.fr  
SNCF Réseau  
Saint-Denis, France

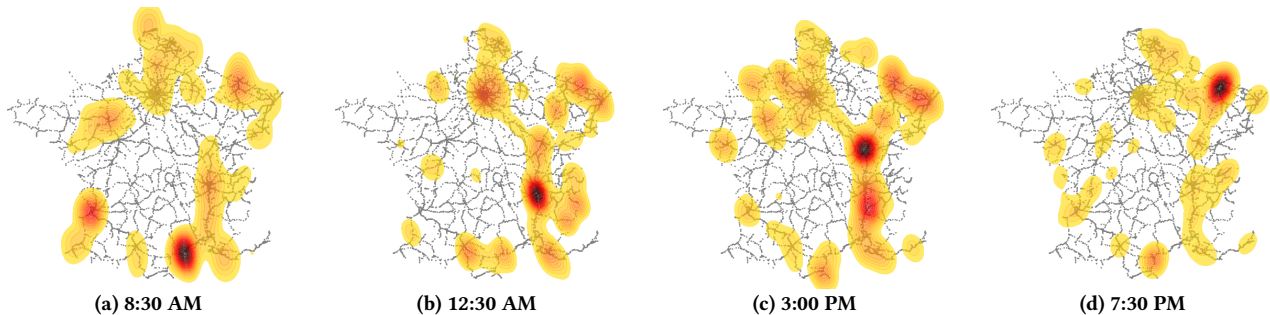


Figure 1: Gaussian density model of train delays on the NRN on March 5<sup>th</sup> 2019, demonstrating delay propagation

## ABSTRACT

Robust travel time predictions are of prime importance in managing any transportation infrastructure, and particularly in rail networks where they have major impacts both on traffic regulation and passenger satisfaction. We aim at predicting the travel time of trains on rail sections at the scale of an entire rail network in real-time, by estimating trains' delays relative to a theoretical circulation plan.

Predicting the evolution of a given train's delay is a uniquely hard problem, distinct from mainstream road traffic forecasting problems, since it involves several hard-to-model phenomena: train spacing, station congestion and heterogeneous rolling stock among others. We first offer empirical evidence of the previously unexplored phenomenon of *delay propagation* at the scale of a railway network, leading to delays being amplified by interactions between trains and the network's physical limitations.

We then contribute a novel technique using the transformer architecture and pre-trained embeddings to make real-time massively parallel predictions for train delays at the scale of the whole rail network (over 3000 trains at peak hours, making predictions at an average horizon of 70 minutes). Our approach yields very positive results on real-world data when compared to currently-used and experimental prediction techniques.

## KEYWORDS

operations research, complex systems, traffic forecasting, propagation forecasting, transformer model, delay propagation

## 1 INTRODUCTION

Delay prediction is one of the most fundamental and oldest computational problems in railway operations. They are important both

to infrastructure operators, as predicting delays can aid in real-time traffic regulation, and to passenger rail operators to improve passenger information and therefore satisfaction [26, 31].

Moreover, the growing scale and interconnectedness of rail networks, as well as the wealth of delay data accumulated by rail companies can make it hard to isolate specific phenomenon which cause delays. Besides *extrinsic delays*, the phenomena causing *delay propagation* have been of particular interest in the literature in recent years [2, 9, 11]. Predicting the evolution of a given train's delay is a uniquely hard problem, distinct from mainstream road traffic forecasting problems, since it involves several hard-to-model phenomena: train spacing, station congestion and heterogeneous rolling stock among others, which can all lead to delay propagation.

We give a succinct description of the **delay propagation** phenomenon in Section 3, wherein late trains will cascade additional delays for other trains. Existing literature often treats these phenomena at a local scale, or isolates each type of phenomenon causing delay propagation (which we outline in Section 3). As explained in Section 3 and Section 4, we treat all causes of delay propagation together, and use massive network-scale predictions to encompass all aspects of delay propagation.

Real-time delay predictions for medium-term horizons are useful for a variety of reasons for railway operators: they feed passenger information systems and they allow network regulators to make more informed decisions. Moreover, the study of delay propagation can also help network operators understand where extraneous delays are created, and help fluidify the network. These real-world requirements translate into a prediction horizon of the order of magnitude of several dozens of minutes, a scale precise enough to make predictions in each train station and major junction visited by a train, and a prediction computation time below a minute (for

real-time use): our approach satisfies all of these real-world usage criteria.

To this end we propose a novel approach based on the transformer architecture and pre-trained embeddings, described in Section 4, providing real-time predictions for all trains on the French national rail network by taking into account propagation at the time scale of 70 minutes on average. The main idea of our work is to make predictions in parallel at the network scale, taking into account all trains’ states when making predictions for a single train, along with an extensive history of every train’s itinerary. We call our method ‘massively parallel’ for this reason: in contrast with existing work, all propagation paths between all trains are considered by our architecture. We finally present our results and compare them experimentally both to currently deployed techniques (our baseline) and a statistical Bayesian network technique in Section 5.

## 2 RELATED WORK

Most work using neural networks for traffic forecasting in transportation networks so far has been focused on road traffic. These tasks typically model average speed on highways (such as the METR-LA and PEMS-BAY datasets) or traffic flow along city streets (BJF and BRJ, Zhang et al. [32]); however these variables are often ill-defined in a railway context: 96.7% of edges of our network never contain more than 4 trains simultaneously, and during peak hour over 97.3% of edges contain no trains. Railways also introduce many constraints that don’t exist for road traffic: incidents have much more propensity to completely halt flow of traffic on most one-way tracks, train spacing strongly limits traffic density, and platform occupancy constraints in stations create unavoidable congestion at specific nodes. The sparsity of train traffic along with the branching structure of railway networks thus make it impossible to apply approaches designed for road traffic, which have a macroscopic view of traffic in contrast with the vehicle-by-vehicle basis required for rail traffic. A closer task to ours is estimating single vehicle travel time within a road network based on congestion information in a city’s network [14, 27]. However, the data used for inference is very different from our rail setting: congestion generally is not the determining factor for delays in rail traffic, and as outlined above is often not well-defined in our problem.

Machine learning has been used to improve traffic predictions for trains. A variety of statistical methods have been suggested to model delay propagation, for example using timed event graphs [9], fuzzy Petri networks [22], activity graphs [3], random forests [20], Bayesian networks [5], and integer programming [8]. Spaninger et al. [25] and Tiong et al. [26] offer detailed and complete reviews of the area, which is not in the scope of this publication. These models are however constrained by scale, modeling propagation from an individual train to another, most often on a single railway line. At the scale of an entire network, as is our case, massive delay propagation as demonstrated in Section 3 would entail a lot of uncertainty using train-to-train propagation as errors would accumulate. Most work so far referring to ‘delay propagation’ limits itself to propagation between the different stops of a single train, or along a single railway line between trains following each other; whereas we account for interactions between all trains, introducing many more propagation paths. Moreover, these works choose to

model each propagation phenomena separately, making way for omissions or imprecisions, whereas our model summarizes all forms of propagation in a single prediction scheme.

Feed-forward neural networks have previously been used to forecast delays for individual trains [6, 12, 15, 21, 23, 31], using variables such as origin and destination of the train and past observed delays. These models are often relatively simple (less than 10k parameters), and don’t account for delay propagation between trains. Bosscha [2] uses recurrent neural networks for single-train delay predictions, incorporating a form of delay propagation between trains by tracking how many trains departed at the same time as a given train. This single variable however fails to capture large-scale delay propagation phenomena we are interested in. Li et al. [19] study propagation at multi-line stations using convolutional neural networks, and contains a partial review of the area of delay forecasting. Their approach focuses on delay propagation at a single railway station: as detailed in Section 3, our approach encompasses many other modes of propagation that may occur outside of train stations, for example between trains which do not share a station. One of the main benefits of our approach is the self-attention mechanism of the transformer architecture, which is not present in feed-forward networks and which we use to capture usual propagation paths between trains. As our task is very different from these works in scale but also in the propagation mechanisms we aim to predict (see Section 3), experimental comparisons would be ill-defined: scaling up existing approaches or scaling down our approach to single trains, stations or lines would require significant modifications to both.

Our work uses the transformer architecture [28] to make delay predictions, a neural network architecture based on a self-attention mechanism first proposed for machine translation. It has since been declined to other neural language processing (NLP) tasks such as language modeling [7]; but also different domains such as computer vision tasks [10] and time series forecasting [18]. Recent work on road traffic forecasting tasks has also used the transformer architecture [4, 30], using attention for spatial and temporal domains. As above, these are not applicable to the rail domain, but validate the relevance of self-attention for propagation forecasting. Cai et al. [4] use transformer inputs for traffic at different times, and deal with the spatial dimension using a graph neural network layer: this is the dual to our approach, where time is encoded as components of the tokens fed to the transformer encoder, and spatiality is captured through the different tokens (each corresponding to a train, see details in Section 4). Xu et al. [30] alternate spatial and temporal encoders, also using graph neural networks to encode spatial data. Once more, our approach avoids the use of graph neural networks (as well as positional encodings in the transformer) by leveraging the fact that spatial features can be passed along discrete train positions, which is not the case in road traffic where individual vehicles are too numerous and hard to locate for such an approach. To the best of our knowledge, no prior work uses the transformer architecture for delay propagation forecasting at the scale of an entire rail network.

### 3 DELAY PROPAGATION

Making predictions for train delays relative to a theoretical circulation plan, given the state of the entire railway network requires to account for a variety of extrinsic and intrinsic factors described below. We distinguish *primary delays*, introduced organically for on-schedule trains, from *secondary delays* (sometimes called *knock-on delays*) which are propagated from or amplified by existing primary delays or degraded circulation conditions.

The following is a coarse and non-exhaustive categorization of the main sources of delays observed on a typical railway network,

- (1) **Extrinsic incidents:** incidents unrelated to previous incidents or the theoretical circulation plan are a primary and unpredictable source of lateness, with 1,250 occurring on average each day on the French national railway network. Examples are animals being present on the tracks or a train breaking down.
- (2) **Inconsistent circulation plan:** imperfections in the circulation plan are also a primary source of delays. This is most often due to an optimistic modelisation of real-world conditions, such as acceleration curves, maximum speeds or passenger loading time. This is visible in our data through recurring biases in delays at specific edges in the network.
- (3) **Race conditions:** a train can accumulate delay based on race conditions at certain railway nodes such as junctions or stations. This is a secondary source of lateness, since it requires for another train to be late in order to occur. Examples include waiting at a signal when it is reached later than scheduled, waiting before a station when a train's allotted platform has become occupied, and traveling at a reduced speed when running behind a slower rolling stock.
- (4) **Traffic regulation decisions:** traffic regulation is done entirely by humans and based on experience foremost. This means that agents' discretion dictates how recovery from an incident is carried out, and human error or misperception might introduce flaws in regulation. This leads to sub-optimal traffic conditions, or exacerbated secondary delays which are hard to predict due to the added human element.
- (5) **Traffic density:** at peak hours, major arteries on the railway network are saturated, meaning train spacing is at a minimum all along the line. If a train comes too close to the train in front of it, automatic signals (KVB in France) will slow it down, leading to accordion effects all along the line. This fragile equilibrium is easily disturbed especially at the end of high-speed sections or at junctions along these lines where trains might enter.
- (6) **Transfers and shared rolling stock:** passenger transfers along important railway nodes can lead to a train being delayed when many of its passengers are coming from a delayed train. Moreover, some services will share rolling stock between trips, creating more opportunities for delay propagation. Crew scheduling conflicts can also worsen delay propagation when extreme delays occur.

Our approach aims to tackle the latter five points, with extrinsic incidents being the sole unpredictable and hard-to-estimate factor. The contributions of the latter four points are what we call **delay propagation**, a phenomenon wherein minor perturbations can

cause major delays on entire sectors of the network by exacerbating weaknesses in the circulation plan and the network's structure. To address this, we emphasize parallel prediction of all trains, with extensive history as input: rather than proceeding line-by-line or station-by-station as most previous work does, our model observes the situation of all trains on the network at once (as well as its history).

Figure 1 contains a concrete example of delay propagation on the French national railway network on a given day. The images depict a Gaussian model of the density of recorded delays over a window of 30 minutes at RPs. This Gaussian density is normalized by the density of RPs, to avoid dense areas (such as Paris) always registering the highest values due to the density of traffic and RPs.

The figures are taken at four different times of the day, the first image at 8:30 AM registers a high density of delays in the south, the second sees it move towards the South-East, then Dijon to the South-East of Paris on the third image. The last image at 7:30 PM finally shows a very high density of delays in Metz in North-Eastern France – it is remarkable that such a minor railway node has a higher concentration of delays than the entire Paris area, most likely due to delay propagation. The full animation shows an even clearer image of the concentration of delays moving along the described trajectory. The delays propagating are not carried by any single train, since no train on that day travels from Perpignan to Metz, and the delay concentration often pauses at major railway nodes such as Lyon. The other concentrations of delays on the map do not follow any clear patterns of delay propagation in this example, and do not seem to interact with the main pole of delays shown in the map.

#### 3.1 Setting

The French National Rail Network (NRN) contains about 10,000 **remarkable points** (RP), each of which are various types of important railway nodes: train stations, junctions, bifurcations, train depots, signals, ... All stations are RPs, but not all junctions are RPs, making it a high-level description of the network which does not account for individual tracks or switches. These points can be considered as nodes of a graph of the rail network, with two remarkable points being connected with an undirected edge if one can be reached from the other. The spacing between two consecutive RPs is very heterogeneous, ranging from a few kilometers within Paris to over 90 km on low-density railways in rural areas.

About 6,000 of these RPs are equipped to communicate with trains when they travel through them, creating a database of all train passages at these RPs. On any given weekday, about 350,000 such events are recorded at *SNCF Réseau*, France's national railway network manager. This database provides a rough description of the NRN's state at any given moment, positioning each train on an edge or node of the network's graph; however providing no information on the trains' precise position along an edge nor their speed or state. This description of the rail network corresponds to the *macro level* defined by the International Rail Solution's RailTopoModel standard [16], which means our approach can be generalized to any network described with this standard.

On the French NRN, most trains follow a pre-established schedule every day called the **circulation plan**, repeated every weekday,

Table 1: Sample of BREHAT data

id	time	RP	type	delay	trainNum
462175827	2018-01-06 09:42:30	681247BV	P	-4	6920
931562731	2018-01-04 20:54:24	11320933	P	111	4453
147732417	2018-01-08 05:20:55	715938WS	O	16	220
108326080	2018-01-01 22:13:22	713339RV	P	7	853221



Figure 2: Representation of RPs superimposed on railways, area surrounding Grenoble and Lyon.

with two alternate versions for Saturdays and Sundays. Trains are each given a **train number**, which for most trains designates a precise itinerary and time schedule, repeated daily. Some exceptional trains do not follow this scheduled plan and are assigned an arbitrary number from a given range, and holidays affect the circulation plan for all trains.

The combination of the NRN state and recently-observed events, as well as historical data about the circulation plan is enough to make informed predictions about how trains will behave in the medium term.

### 3.2 Data

Our data consists of raw **observation events** contained in a database called **BREHAT** at *SNCF*. The database is built in real-time from beacons on the network and the circulation plan, and has been recorded for the past 10 years. Each observation in the database contains the following information: time of observation; remarkable point where the train flagged the beacon; observation type, a categorical variable among *O* for origin, *T* for terminus, *P* for passage (without stopping), *A* for arrival at a station and *D* for departure from a station; train number indicating the train’s service; and measured delay relative to the theoretical circulation plan.

Table 1 shows a sample of **BREHAT** data. The measured delay variable can be used to reconstruct the up-to-date circulation plan by subtracting delays from observation times. Train numbers contain a lot of information about each train, such as its region

and itinerary, rolling stock type, and whether it is traveling in one direction or the other along the itinerary.

### 3.3 Existing approaches

The **BREHAT** database is occasionally flawed due to dysfunctional equipment on the network and inaccuracies in the circulation plan, leading to both random and repeated drop-out for events. These inconsistencies in the data, as well as its aforementioned coarseness, make it impossible to accurately simulate the rail network’s evolution. Doing so would require additional data regarding rail structure at a lower scale than RPs (signal position and state), physical information about rolling stock (acceleration and deceleration curves), and extrinsic information such as driver behavior. This makes approximation based on past behavior the most rational approach, preferably modeling all of the delay phenomena listed at the beginning of this section together rather than separately.

*Translation.* Our baseline approach is called **translation**, which predicts the most recently observed delay for all following RPs on the train’s itinerary. Translation therefore assumes that a late train will neither catch up its delay, nor accumulate any further delays, making it a very simple yet remarkably accurate approach to delay forecasting. This is the currently used technique at *SNCF* both for passenger information and traffic control, meaning that phenomena such as race conditions are never accounted for in predictions as each train is treated individually and independently of its position or state. Moreover, since translation only accounts for the *last measured* delay, a train accumulating a large delay between two RPs will not be detected as late until it reaches the next RP.

*ARMA and ascendancy graphs.* Autoregressive–moving-average (ARMA) models are a widely-used class of models for time series prediction. Within *SNCF*, a first improvement attempt over translation uses control theory and a conductor/train dynamic [24] wherein a driver attempts to follow a schedule while the train has an opposing effect, yielding an AR(2) model [29] for delays:

$$\epsilon(n) = \alpha\epsilon(n-1) + \beta\epsilon(n-2) + \gamma. \quad (1)$$

The parameters  $\alpha, \beta, \gamma$  are fit for each train trajectory. Experiments at the scale of single train lines failed to surpass translation’s general performance, but yielded very positive results for data filtering and smoothing by using an orthogonal projection and low-pass filtering technique. This model, which doesn’t account for propagation between trains, was compared to an approach using adjacency graphs and small fully connected and convolutional neural networks [24]. An ascendancy graph is built for each train and RP pair  $(t, r)$ ; and nodes are created for the  $n$  previous trains going through  $r$ . Edges are weighted according to the time difference between the trains at  $r$ , and the Laplacian matrix for the graph is interpreted

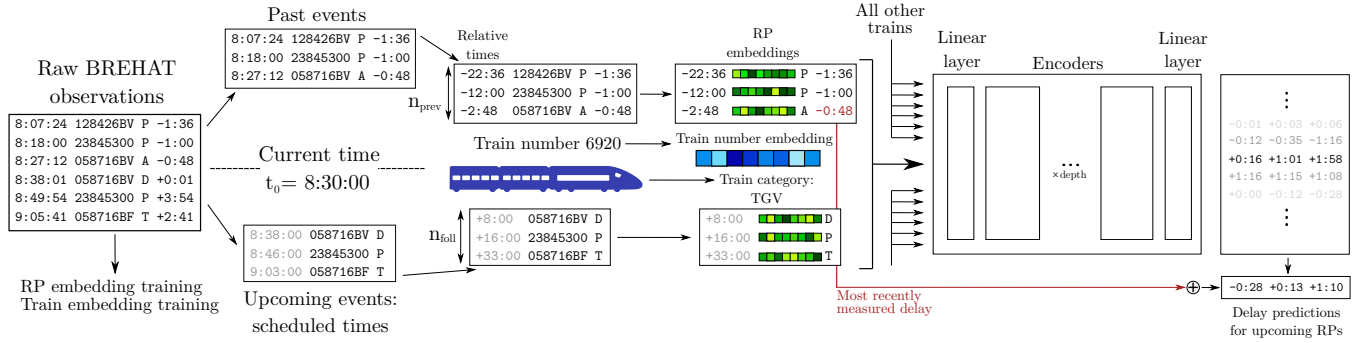


Figure 3: Summary of our prediction system

as an image by the network. These experiments failed once more to outperform translation but demonstrated capability to model interactions between trains.

*Bayesian networks.* Another approach previously explored at SNCF are Bayesian networks [5], which model each pair of train number and RP  $(t, r)$  as a node in a directed acyclic graph weighted according to the historical correlation between delay at the target node and at the source node. The resulting graph, containing over 300,000 nodes, is thinned to only contain physically meaningful edges: an edge is kept if the target node chronologically occurs after the source node; and both nodes relate either to the same train, same RP, or both occur within a given window of time. The weights of edges designate how the delay from the source train at the source RP affects the target train at the target RP, and are learned through historical correlation of these delays. If we denote  $L(x)$  the delay stored at node  $x$ , either the actual measured delay if it has already occurred, or the prediction if it has not, then predictions for a given node  $x$  are recursively defined as,

$$L(x) = b(x) + \sum_{y \text{ parent of } x} w(y, x)L(y), \quad (2)$$

where  $w(y, x)$  are the learned weights through past observed correlation of delay at  $y$  and  $x$ ; and  $b$  a learned parameter for each node. This approach is the simplest and most natural when considering spatio-temporal propagation of delays, since it should capture delays being propagated from a train to another by the phenomena described earlier, albeit only in a linear fashion.

## 4 TRANSFORMER-BASED APPROACH

Our system performs real-time predictions for all trains on the network, in parallel, taking into account delay propagation. For this, we first pre-process BREHAT data to simulate real-time predictions for training. This data is also used to create two pre-trained embeddings using auxiliary neural networks, to embed the RPs and train numbers into meaningful variables as inputs for the neural network. The main model, based on the transformer architecture, processes each of these embedded train vectors as separate tokens of its input and outputs predictions for all trains at once. The training set-up for our system is summarized in Figure 3.

### 4.1 Preprocessing

Given a point in time  $t_0$ , our experimental set-up emulates real-time conditions from historical BREHAT data, by reconstructing the theoretical circulation plan used when populating the database. Events occurring before  $t_0$  are used as-is, whereas events occurring after  $t_0$  are only used to extract information about the theoretical circulation plan: RPs to be visited, types of observations to be done, and scheduled time for these events (by adding delay to observation time). This means there is no information leakage from events occurring after  $t_0$ , even if they were scheduled to occur before  $t_0$ .

Our main model takes as input a list of trains on the network, in the form of embeddings for each train containing information on their previous itinerary, and upcoming itinerary. This information is given to a horizon of  $n_{\text{prev}}$  RPs for the past itinerary and the  $n_{\text{follow}}$  RPs for the upcoming itinerary. For each train, the following information is encoded as a vector and fed to the main model:

- The train category: high-speed, regional, freight... encoded as one-hot
- The embedding of the train number (see Subsection 4.3)
- The embedding of the  $n_{\text{prev}}$  previous RPs visited by the train (see Subsection 4.2)
- The time elapsed since each of these RPs were visited
- The measured delay at each of these RPs
- The embedding of the  $n_{\text{follow}}$  next RPs to be visited, and their scheduled time of arrival
- The observation type of past and upcoming RPs encoded as one-hot
- Exogenous variables providing context for predictions: day of week, time of day, and number of trains on network.

All trains currently traveling on the network are included as inputs to the model, but also those that have arrived less than the  $h_{\text{arr}}$  arrival horizon ago, or will leave in less than the  $h_{\text{dep}}$  departure horizon. Including these trains has several benefits, it allows the model to use data about trains that have already arrived to better understand the state of the network. Including arrived trains helps understand delay propagation through traffic regulation decisions and shared rolling stock and transfers as described in points (4) and (6) in Section 3. Including trains that depart soon produces predictions for trains that haven't left yet, which is important for passenger information and regulation planning purposes, given these trains may also suffer delays through propagation.

In the case of trains that have not yet departed or already arrived (or recently departed or arrived), it is necessary to pad the information on past or future RPs beyond  $n_{\text{prev}}$  or  $n_{\text{full}}$ . For this purpose, we introduce two stand-in RPs labeled `preDeparture` and `postArrival` to fill in embeddings. All other information (observed delay, time elapsed since RP, ...) for these stand-in RPs is arbitrarily set.

## 4.2 Remarkable point embedding

Remarkable points given as input to the model as part of the train’s itinerary must contain easily-retrievable information about the graph structure of the NRN for the model to be able to predict whether two given trains will visit near-by nodes and potentially interact. This information can be encoded in an appropriate graph embedding for the NRN, which must account for heterogeneous travel times along edges and local graph structure.

To this end, we pre-train our RP embedding on a side task which also uses the graph structure of the network, in this case **itinerary length estimation**. Given two RPs as their embeddings, a small neural network must estimate the length in minutes of the shortest path connecting them, as well as the number of RPs on this path. The embeddings are considered as variables in the gradient descent algorithm and are thus trained at the same time as the neural network.

For this, we used historical data to build median travel times between two given RPs in the NRN, regardless of rolling stock, and use a shortest-path algorithm to create training data. We also reduce the NRN to its connected components prior to this, as some parts of the network are fully grade-separated. It is important this network be small enough to avoid over-fitting, and train the embeddings so the information is as easily-retrievable as possible by the main model. In our experiments, the network used for training is a simple fully-connected network of depth 2 and hidden dimension 64<sup>1</sup> using PReLU<sup>2</sup> non-linearities [13]. Outputs are normalized and training performed using the  $\ell^2$  loss and the Adam optimizer [17].

## 4.3 Train number embedding

It is also important to encode the information from train numbers in a meaningful manner. To this end, we use the side task of **itinerary prediction**: given the embedding of a train’s number and the embedding of an RP, a small neural network must predict the next RP visited by the train. This associates train numbers to RP itineraries, and if this information is correctly embedded, it allows the main model to look ahead to which trains are likely to occupy the same RPs in the network. In order to force generalization and emphasize the importance of train numbers we add a random drop-out where the current RP is randomly hidden. Predictions are also sometimes randomly compared to two RPs ahead, or to the previous RP<sup>3</sup>.

<sup>1</sup>A fully-connected network is a series of linear transformations alternating with non-linear transformations. Its depth refers to the number of linear transformations in the network, and the hidden dimension is the dimension to which the first linear transformation maps the input vector.

<sup>2</sup>A ReLU non-linearity is the function  $x \mapsto \max(x, 0)$ . A leaky ReLU is a ReLU non-linearity with a small coefficient applied to negative values, i.e. the class of functions  $x \mapsto \epsilon x \mathbb{1}_{x < 0} + x \mathbb{1}_{x \geq 0}$ . A PReLU non-linearity is a parametrized leaky ReLU non-linearity with a learnable slope parameter  $\epsilon$ , i.e. where  $\epsilon$  is a parameter that is learned through gradient descent as well.

<sup>3</sup>In particular, this means the output is not a deterministic function of the inputs.

In summary, given a batch of train numbers  $t_i$  and RPs  $r_i$  respectively visited by those trains and their respective ranks on the trains’ itineraries  $k_i$ , define conditionally independent random variables  $x_i$  of Bernoulli law of probability  $p$ ; and random independent variables  $n_i$  taking values  $-1, 1$  and  $2$  with probabilities  $q_{-1}, q_1$  and  $q_2$  respectively. Denoting the cross-entropy loss  $\mathcal{L}$ , the batched loss used for the model  $f$  is then defined as,

$$l((t, r), f) = \sum_i \mathcal{L}(f(t_i, x_i \cdot r_i), R(t_i, k_i + n_i)) \quad (3)$$

where  $R(t_i, k_i) = r_i$ ,

and where  $R$  contains the RPs visited by each train with padding:

$$R(t, k) = \begin{cases} \text{preDeparture} & \text{if } k < 0 \\ \text{postArrival} & \text{if } k > N_{\max}(t) \\ k^{\text{th}} \text{ RP visited by } t & \text{otherwise.} \end{cases} \quad (4)$$

The labels `preDeparture` and `postArrival` denote two arbitrary vectors that designate virtual RPs that act as placeholders before a train starts its itinerary or after they arrive.

In our experiments, we set  $p = 0.15$  and the vector  $(q_{-1}, q_1, q_2) = (0.07, 0.75, 0.18)$  and use the Adam optimizer [17]. The network is made of two fully-connected layers of dimension 256, with a PReLU non-linearity (see definition in previous section).

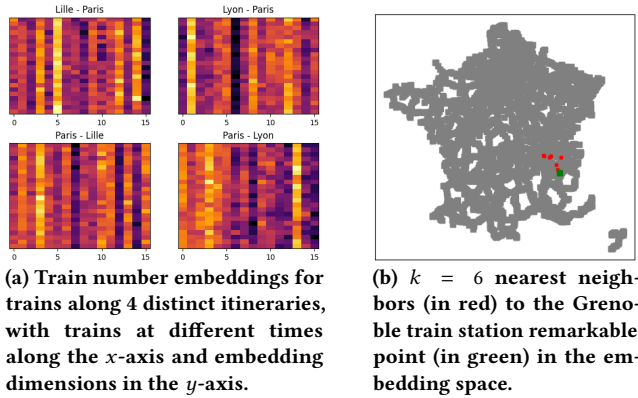
Visualizations and interpretations for our embeddings are presented below in Subsection 4.4, and help set hyperparameters for the embeddings dimension and avoid over- and under-fitting. For instance, setting the dimension for RP embeddings to  $d_{\text{RP}} = 16$  gives our embeddings too much entropy and the  $k$ -closest neighbors for a given RP are spread out across France: the model has over-fit the embeddings and they no longer contain geographical information. Inversely, setting this dimension to 4 lost too much information and made the itinerary length prediction model ineffective.

## 4.4 Embedding interpretability

In order to avoid adopting a black box end-to-end approach, as well as to aid with selection of hyperparameters (as explained in the previous subsection), we verify the interpretability of the trained embeddings on three different techniques illustrated in Figure 4:

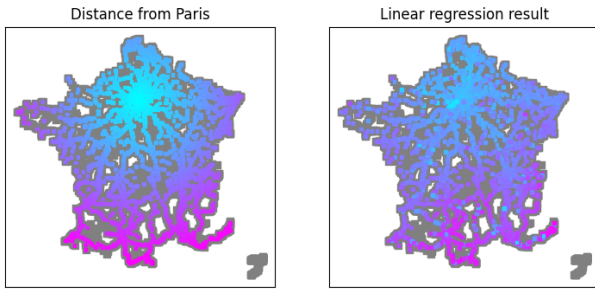
- Train numbers that travel along the same itinerary at different times should have similar embeddings, shown here by plotting embeddings for each train on a specific itinerary at a different time on each line. Columns are the different components of the  $d_{\text{train}} = 16$  dimensions in the embedding, and lines are different train numbers for the same itinerary.
- Near-by RPs should have similar embeddings, illustrated here using the  $k$ -nearest neighbors (shown in red) for the Grenoble train station RP (shown in green) in the embedding space: this ensures that no over-fitting has taken place and that near-by RPs for railway distance are indeed near-by in the embedding space.
- Physical location of RPs should be easily extractable from their embeddings, as illustrated here using linear least-squares regression to recover geographical distance from Paris from the embeddings.

All of these illustrations provide good reasons to believe the embeddings faithfully encode information about the rail network,



(a) Train number embeddings for trains along 4 distinct itineraries, with trains at different times along the  $x$ -axis and embedding dimensions in the  $y$ -axis.

(b)  $k = 6$  nearest neighbors (in red) to the Grenoble train station remarkable point (in green) in the embedding space.



(c) On the left, the distance of remarkable points from Paris according to a color scale. On the right, the result of a linear regression on the remarkable point embeddings to recover this distance.

Figure 4: Three visualizations of interpretability of our embeddings.

and the trains' schedules. They were also very useful in setting the embeddings' hyperparameters such as dimension and training parameters, by providing an *a priori* measure of their effectiveness without re-training a complete transformer model.

#### 4.5 Transformer encoder model

Our main model is the succession of a linear layer, a transformer encoder stack, and another linear layer. The details for the architecture of transformer encoders are explained in detail in Vaswani et al. [28]. The first linear layer shapes each train's embedded vector into the right dimension for the encoders. Each train's vector after this layer is used as a parallel input to the encoder stack, similarly to a token in a sentence fed to an NLP model. After the stack of encoders, another linear layer converts the output to the right dimension for the delay predictions. Subsection 4.6 provides more insight into the behavior of self-attention in our task and the rationale behind the use of this architecture.

The output, of dimension  $n_{\text{trains}} \times n_{\text{fo}}ll$ , represents predictions for the next RPs for all trains. Outputs for the postArrival RP are discarded when computing the batched loss, since they do not represent real measured delays. All numeric inputs (times and delays but not embeddings) to the model and all model outputs are normalized using the empirical mean and standard deviation of the training data, in order to accelerate training. Before normalizing,

we also convert all delays to their square roots and then take the square of all output delays before un-normalizing: by working in square root space, the model is less sensitive to big delays, which avoids few very late outlier trains taking more importance than the rest. Therefore, if the delays as input are  $d_{-n_{\text{prev}}}, \dots, d_{-1}$  and times are  $t_{-n_{\text{prev}}}, \dots, t_{n_{\text{fo}}ll-1}$ , they will be transformed by  $f$  before and  $f^{-1}$  after the first and final linear layers of our model:

$$f(x) = \text{sgn}(x)\sqrt{|x|} \quad (5)$$

$$f^{-1}(y) = \text{sgn}(y)y^2 = |y| y. \quad (6)$$

Our experiments also present a model using the logarithm and exponential functions in place of the square root here, and another using the identity function for  $f$  and  $f^{-1}$ .

Finally, rather than using the output directly as a prediction, we add the translated delay to all predictions. The translated delay is the last measured delay for the train, meaning that our model predicts the difference between the last measured delay and the real delay. We chose to clip predictions that would lead for an unreached RP to be predicted in the past: we apply a ReLU non-linearity<sup>4</sup> to the prediction added to the scheduled remaining time, before subtracting the scheduled time again; effectively clipping all predictions to the current time. This post-processing step is only used when testing the model but not during training, in order to still correct these harmful predictions and improve performance – doing so during training would prevent the model from learning from these mistakes through gradient descent.

To summarize, given a train  $i$  and the index of an upcoming RP  $j \leq n_{\text{fo}}ll$ , denote  $y_{i,j}$  the model's raw output,  $\mu, \sigma$  the mean and standard deviation of training data,  $t_{i,-1}$  the last measured delay for the train, and  $s_{i,j}$  the scheduled remaining time to the RP (potentially negative when the train is late), then our prediction is,

$$\sigma f^{-1}(y_{i,j}) + \mu + t_{i,-1} \quad \text{when training} \quad (7)$$

$$\max\left(\sigma f^{-1}(y_{i,j}) + \mu + t_{i,-1} + s_{i,j}, 0\right) - s_{i,j} \quad \text{when evaluating.} \quad (8)$$

#### 4.6 Self-attention between trains

There are two strong rationales for using a transformer-based architecture for this task. The first is that we are confronted with a long list of input tokens, of variable length: the main alternative would have been recurrent neural networks (such as bi-directional LSTMs), but this would raise questions about token ordering and memory length to process over 3,000 train tokens as input.

The second rationale is the attention mechanism, which allows the model to focus solely on relevant trains when making a prediction for a given train. Self-attention works by transforming each input token  $x$  into query  $Qx$ , key  $Kx$ , and value  $Vx$  vectors in each attention head [28]. Then, each token  $y$  is weighted relative to  $x$  through the scalar product  $(Qx) \cdot (Ky)$ . These weights are normalized using a soft-max layer and then these scores used to produce a convex combination of each token's value vector,

$$A(x) = \sum_y \mathcal{S}((Qx) \cdot (Ky)) Vy, \quad (9)$$

<sup>4</sup>A ReLU non-linearity is the function  $x \mapsto \max(x, 0)$ .

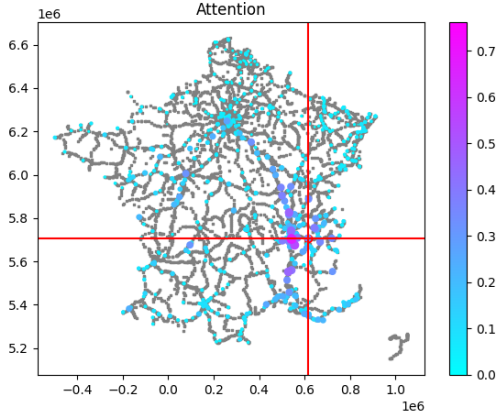


**Figure 5: Self-attention in the first encoder for predicting delays for a Grenoble-Paris TGV shortly after leaving.**

which will constitute the output for token  $x$ , where  $S$  is the soft-max function relative to the weights.

We are interested in the normalized weights  $(S((Qx) \cdot (Ky)))_y$ , which constitute a probability distribution over all trains in the input, modeling the way they affect the train  $x$  in each self-attention layer. We therefore chose to monitor alongside our performance metrics the attention weights for the first encoder in our stack. This information is extremely valuable since it roughly encodes how delays propagate: if a model pays particular attention to a set of trains when making a prediction for a particular train, this most likely means that these trains are likely to impact the second train.

While this cannot be quantitatively evaluated, visual analysis of snapshots of the model’s attention yields very interesting results. Figure 5 shows the attention for a high-speed train leaving from Grenoble to Paris, situated at the intersection of the two red lines. Each colored point represents another train on the network at the time, whereas gray points are RPs. The size and color scale of points quantifies the weight of the self-attention vector when evaluating the train leaving Grenoble, hence how important they are in the first encoder block of the model for predicting the delay of the train from Grenoble to Marseilles. The train is about to join the high-speed line from Marseilles to Paris, and the figure shows the model’s attention is focused on other trains coming from Marseilles which are already on the high-speed line. This is likely what a human operator would also predict, since these trains are the trains that will also be traveling on the high-speed line between Lyon and Paris, demonstrating in this example that the model is capable of distinguishing relevant from irrelevant trains when making a prediction.

These self-attention figures can be of independent interest to train operators in better understanding the source of delay predictions, and more generally the mechanisms underlying delay propagation.

## 5 EXPERIMENTS

We present two experiments, one small preliminary experiment trained on two months of data to compare our approach to Bayesian networks; and another large-scale experiment trained on two and

a half years of data and tested on three months of data. This distinction is made due to the conclusive results of the preliminary experiment, and computation considerations for the training of Bayesian networks. All of our models are implemented using the PyTorch library.

We clean **BREHAT** data for simple inconsistencies such as duplicate observations or permutations in the order of events. We remove all local passenger trains for the Île-de-France region (around Paris), as they constitute a large proportion of data (about a third of observations, due to traffic and RP density) but are mostly grade-separated from the rest of traffic. These trains can thus be treated separately, reducing the amount of tokens as input to our model. Our final database of observation events contains about 142M events for the three years, which averages to 142,000 events a day and 7,500 trains a day. We then create regularly-spaced training points as described in Subsection 4.1 for each day between 6 AM and 11 PM, 15 minutes apart for training days and 4 minutes apart for test days. Appendix A.2 describes data released for reproducibility purposes.

The number of trains as input to our model varies on a normal weekday between 1,000 in the evening and 3,000 during morning and afternoon peak hours. The average delay for observations is 5 minutes, the median 0 minutes and the standard deviation 27 minutes: most trains are on time (or early), but late trains introduce a lot of variation in measured delays.

We set  $n_{\text{prev}} = 10$  and  $n_{\text{foll}} = 40$ , and the depth of our encoder stack is 2, as experiments with deeper stacks yielded no major improvements. Our transformer model has dimension  $d_{\text{model}} = 1024$ , a feed-forward dimension of  $d_{\text{ff}} = 4096$ ,  $h = 2$  heads in each self-attention layer, and a dropout probability of  $P_{\text{drop}} = 0.1$  using notation from Vaswani et al. [28]. Our chosen embedding dimensions are  $d_{\text{RP}} = 12$  and  $d_{\text{train}} = 16$ , and were set according to the interpretability visualizations explained in Subsection 4.3. We use horizons  $h_{\text{arr}} = 90$  minutes and  $h_{\text{dep}} = 12$  minutes, chosen to minimize the number of trains while conveying enough information about recently-arrived or departed trains.

Our model is trained using the Adam optimizer [17] at a learning rate of  $5 \times 10^{-5}$  and a batch size of 32, using the L1 loss. All models are trained on a system using a single NVIDIA Tesla T4 GPU. The main model was trained over the course of approximately 24 hours.

### 5.1 Evaluation

The two first presented metrics are Mean Average Error (MAE) and Mean Square Error (MSE). Mean average error refers to the average  $\ell^1$  error, i.e.  $\frac{1}{N} \sum_i |\text{predicted}_i - \text{real}_i|$  where  $i$  varies over the  $N$  observations of the experiment. Mean squared error refers to the average  $\ell^2$  error, i.e.  $\frac{1}{N} \sum_i (\text{predicted}_i - \text{real}_i)^2$ . We use on top of this two non-differentiable **passenger information reliability** metrics which are already in use within *SNCF*: MSE will tend to emphasize errors on large, unpredictable delays, whereas MAE has a more uniform focus on all types of errors.

We use on top of this two non-differentiable **passenger information reliability** metrics which are already in use within *SNCF*:

- i the **incident metric** requires our model to make a prediction for the rest of the train’s visited stations within 10 minutes of the first measured delay of at least 5 minutes ;



**Table 2: Results on the preliminary and main experiments**

	Preliminary	Main experiment			
	MAE (↓)	MAE (↓)	MSE (↓)	Incident (↑)	Service (↑)
Translation	2.4	5.6	22.7	77.1	76.3
Bayesian network	2.1	–	–	–	–
Transf. $d = 512$ , no-norm	<b>1.7</b>	4.2	15.2	80.1	77.0
Transf. $d = 512$ , log-norm	–	4.1	15.1	79.8	<b>77.1</b>
Transf. $d = 1024$ , sqrt-norm	–	<b>3.7</b>	<b>14.3</b>	<b>81.2</b>	<b>77.1</b>

- ii the **service metric** requires our model to make a prediction for each of the train’s visited stations 30 minutes before being scheduled there, for all trains.

Both of these metrics only make sense for passenger trains, since other trains do not stop at stations, and the incident metric only applies to trains that record at least 5 minutes delay at any point on their trip. The metrics are given as a percentage of predictions accurate within 5 minutes. In-use systems using human operators and translation score between 60% to 70% for these metrics.

## 5.2 Results

The results for the preliminary and full experiment are listed in Table 2. We present two additional, earlier iterations of the transformer model on our main experiment: both use encoder dimension  $d_{\text{model}} = 512$ , one uses the identity function and the other the logarithm function when pre and post-processing delays and times as explained in Subsection 4.5.

The preliminary experiment delivers a very decisive result concerning the transformer approach. While Bayesian networks were able to account for some of the translation’s shortcomings, the transformer approach clearly has an edge over both. Since translation captures non-propagated delays, any gains over translation are gains due to delay propagation prediction. Therefore, while the absolute difference of Bayesian networks and transformers compared to translation might seem modest, the relevant indicator is the relative gain: the transformer sees more than double the improvement over translation that Bayesian network had.

The main experiment shows further gains in the MAE metric for our main transformer model, with some improvement between the first and final iterations. We also note a benefit to using the square root space when dealing with delays and times in our model, especially on the MSE metric.

We were surprised to notice that the service metric is somehow less improved between iterations of the transformer, even when compared to translation. Our interpretation of this result is that most trains either run on-time and will thus automatically be counted as correct guesses (the 76.3% for translation), or accumulate a great deal of unpredictable primary delay right before the station (the remaining 22.9%). A better metric for propagation is the incident metric, where the model is allowed to measure a first delay on the train before making predictions. It might seem counterintuitive that this metric is measured higher than the service metric for all models, but this can be explained by the fixed horizon of the service metric: many of the predictions for the incident metric will be done less than 30 minutes before a station. This metric

sees a large improvement between models and over translation, indicating our model is capable of modeling propagation between trains, specifically how a late train will increase its delay through the various effects listed in Section 3.

## 6 CONCLUSION

We present the phenomenon of delay propagation at the scale of the national rail network, and detail several factors contributing to it. We contribute a system that accounts for this propagation when forecasting delays for trains, based on the transformer architecture and using pre-trained embeddings. This technique can be applied to any rail network using the RailTopoModel standard [16], which is the case of several European countries’ national networks. We believe the work could be applied at different scales, such as a mesoscopic scale, however this would imply a moderate to high computational overhead. We also offer a rationale for the use of self-attention and massively parallel predictions rather than per-train forecasting as suggested in previous work, along with visual interpretations for the result of self-attention produced by our model. This model surpasses by a wide margin both our baseline, translation, and various other techniques attempted in previous work.

## ACKNOWLEDGMENTS

The authors would like to thank Vianney Perchet and Francis Bach for their precious supervision and feedback. We would also like to thank Amine Chaker and Tom Rousseau for sharing their work with us. Finally, the authors thank Bertrand Houzel and Loïc Hamelin at DGEX Solutions for making this work possible.

## REFERENCES

- [1] Farid Arthaud. 2023. *Sample of BRÉHAT traffic data*. <https://doi.org/10.17632/ft62gkx5tt.2>
- [2] Edwin Bosscha. 2016. *Big data in railway operations: Using artificial neural networks to predict train delay propagation*. Master’s thesis. University of Twente.
- [3] Thorsten Büker and Bernhard Seybold. 2012. Stochastic modelling of delay propagation in large networks. *Journal of Rail Transport Planning & Management* 2, 1-2 (2012), 34–50.
- [4] Ling Cai, Krzysztof Janowicz, Gengchen Mai, Bo Yan, and Rui Zhu. 2020. Traffic transformer: Capturing the continuity and periodicity of time series for traffic forecasting. *Transactions in GIS* 24, 3 (2020), 736–755.
- [5] Amine Chaker. 2020. *Modéliser la propagation des retards dans le réseau ferroviaire*. Master’s thesis. Ecole polytechnique, SNCF.
- [6] X Chapuis. 2017. Arrival time prediction using neural networks. In *7th International Conference on Railway Operations Modelling and Analysis. International Association of Railway Operations Research, Lille (France)*. 1500–1510.
- [7] Jacob Devlin, Ming-Wei Chang, Kenton Lee, and Kristina Toutanova. 2019. BERT: Pre-training of Deep Bidirectional Transformers for Language Understanding. In *Proceedings of the 2019 Conference of the North American Chapter of the Association for Computational Linguistics: Human Language Technologies, Volume 1*

- (*Long and Short Papers*). Association for Computational Linguistics, Minneapolis, Minnesota, 4171–4186. <https://doi.org/10.18653/v1/N19-1423>
- [8] Twan Dollevoet, Dennis Huisman, Marie Schmidt, and Anita Schöbel. 2018. *Delay Propagation and Delay Management in Transportation Networks*. Springer International Publishing, Cham, 285–317. [https://doi.org/10.1007/978-3-319-72153-8\\_13](https://doi.org/10.1007/978-3-319-72153-8_13)
- [9] Rob M.P. Goverde. 2010. A delay propagation algorithm for large-scale railway traffic networks. *Transportation Research Part C: Emerging Technologies* 18, 3 (2010), 269 – 287. <https://doi.org/10.1016/j.trc.2010.01.002> 11th IFAC Symposium: The Role of Control.
- [10] Kai Han, Yunhe Wang, Hanting Chen, Xinghao Chen, Jianyuan Guo, Zhenhua Liu, Yehui Tang, An Xiao, Chunjing Xu, Yixing Xu, Zhaohui Yang, Yiman Zhang, and Dacheng Tao. 2021. A Survey on Visual Transformer. arXiv:2012.12556 [cs.CV]
- [11] Steven Harrod, Fabrizio Cerreto, and Otto Anker Nielsen. 2019. A closed form railway line delay propagation model. *Transportation Research Part C: Emerging Technologies* 102 (2019), 189 – 209. <https://doi.org/10.1016/j.trc.2019.02.022>
- [12] Florian Hauck and Natalia Kliewer. 2020. Data analytics in railway operations: Using machine learning to predict train delays. In *Operations Research Proceedings 2019: Selected Papers of the Annual International Conference of the German Operations Research Society (GOR), Dresden, Germany, September 4-6, 2019*. Springer, 741–747.
- [13] Kaiming He, Xiangyu Zhang, Shaoqing Ren, and Jian Sun. 2015. Delving Deep into Rectifiers: Surpassing Human-Level Performance on ImageNet Classification. In *Proceedings of the 2015 IEEE International Conference on Computer Vision (ICCV) (ICCV '15)*. IEEE Computer Society, USA, 1026–1034. <https://doi.org/10.1109/ICCV.2015.123>
- [14] Huiting Hong, Yucheng Lin, Xiaoqing Yang, Zang Li, Kung Fu, Zheng Wang, Xiaohu Qie, and Jieping Ye. 2020. HetETA: Heterogeneous Information Network Embedding for Estimating Time of Arrival. In *Proceedings of the 26th ACM SIGKDD International Conference on Knowledge Discovery & Data Mining (Virtual Event, CA, USA) (KDD '20)*. Association for Computing Machinery, New York, NY, USA, 2444–2454. <https://doi.org/10.1145/3394486.3403294>
- [15] Ping Huang, Chao Wen, Liping Fu, Javad Lessan, Chaozhe Jiang, Qiyuan Peng, and Xinyue Xu. 2020. Modeling train operation as sequences: A study of delay prediction with operation and weather data. *Transportation research part E: logistics and transportation review* 141 (2020), 102022.
- [16] IRS. 2016. *RailTopoModel - Railway infrastructure topological model*. Retrieved Jan 29, 2021 from [http://www.railtopomodel.org/en/download/irs30100-apr16-7594BCA1524E14224D0.html?file=files/download/RailTopoModel/180416\\_uic\\_irs30100.pdf](http://www.railtopomodel.org/en/download/irs30100-apr16-7594BCA1524E14224D0.html?file=files/download/RailTopoModel/180416_uic_irs30100.pdf)
- [17] Diederik P. Kingma and Jimmy Ba. 2015. Adam: A Method for Stochastic Optimization. In *3rd International Conference on Learning Representations, ICLR 2015, San Diego, CA, USA, May 7-9, 2015, Conference Track Proceedings*, Yoshua Bengio and Yann LeCun (Eds.). <http://arxiv.org/abs/1412.6980>
- [18] Shiyang Li, Xiaoyong Jin, Yao Xuan, Xiyou Zhou, Wenhu Chen, Yu-Xiang Wang, and Xifeng Yan. 2019. Enhancing the Locality and Breaking the Memory Bottleneck of Transformer on Time Series Forecasting. In *Advances in Neural Information Processing Systems*, H. Wallach, H. Larochelle, A. Beygelzimer, F. d'Alché-Buc, E. Fox, and R. Garnett (Eds.), Vol. 32. Curran Associates, Inc., 5243–5253. <https://proceedings.neurips.cc/paper/2019/file/6775a0635c302542da2c32aa19d86be0-Paper.pdf>
- [19] Zhongcan Li, Ping Huang, Chao Wen, Xi Jiang, and Filipe Rodrigues. 2022. Prediction of train arrival delays considering route conflicts at multi-line stations. *Transportation Research Part C: Emerging Technologies* 138 (2022), 103606.
- [20] ZhongCan Li, Chao Wen, Rui Hu, Chuanlin Xu, Ping Huang, and Xi Jiang. 2021. Near-term train delay prediction in the Dutch railways network. *International Journal of Rail Transportation* 9, 6 (2021), 520–539.
- [21] Nikola Marković, Sanjin Milinković, Konstantin S. Tikhonov, and Paul Schonfeld. 2015. Analyzing passenger train arrival delays with support vector regression. *Transportation Research Part C: Emerging Technologies* 56 (2015), 251 – 262. <https://doi.org/10.1016/j.trc.2015.04.004>
- [22] Sanjin Milinković, Milan Marković, Slavko Vesković, Miloš Ivić, and Norbert Pavlović. 2013. A fuzzy Petri net model to estimate train delays. *Simulation Modelling Practice and Theory* 33 (2013), 144 – 157. <https://doi.org/10.1016/j.simpat.2012.12.005> EUROSIM 2010.
- [23] Luca Oneto, Emanuele Fumeo, Giorgio Clerico, Renzo Canepa, Federico Papa, Carlo Dambra, Nadia Mazzino, and Davide Anguita. 2018. Train delay prediction systems: a big data analytics perspective. *Big data research* 11 (2018), 54–64.
- [24] Tom Rousseau. 2019. *Graphes pour la prédiction de retards*. Master’s thesis. Ecole Normale Supérieure Paris-Saclay, SNCF.
- [25] Thomas Spanninger, Alessio Trivella, Beda Büchel, and Francesco Corman. 2022. A review of train delay prediction approaches. *Journal of Rail Transport Planning & Management* 22 (2022), 100312.
- [26] Kah Yong Tiong, Zhenliang Ma, and Carl-William Palmqvist. 2023. A review of data-driven approaches to predict train delays. *Transportation Research Part C: Emerging Technologies* 148 (2023), 104027.
- [27] Luan Tran, Min Y. Mun, Matthew Lim, Jonah Yamato, Nathan Huh, and Cyrus Shahabi. 2020. DeepTRANS: A Deep Learning System for Public Bus Travel Time Estimation Using Traffic Forecasting. *Proc. VLDB Endow.* 13, 12 (Aug. 2020), 2957–2960. <https://doi.org/10.14778/3415478.3415518>
- [28] Ashish Vaswani, Noam Shazeer, Niki Parmar, Jakob Uszkoreit, Llion Jones, Aidan N Gomez, Ł ukasz Kaiser, and Illia Polosukhin. 2017. Attention is All you Need. In *Advances in Neural Information Processing Systems*, I. Guyon, U. V. Luxburg, S. Bengio, H. Wallach, R. Fergus, S. Vishwanathan, and R. Garnett (Eds.), Vol. 30. Curran Associates, Inc., 5998–6008. <https://proceedings.neurips.cc/paper/2017/file/3f5ee243547dee91fbd053c1c4a845aa-Paper.pdf>
- [29] Peter Whittle. 1951. *Hypothesis testing in time series analysis*. Vol. 4. Almqvist & Wiksells boktr.
- [30] Mingxing Xu, Wenrui Dai, Chunmiao Liu, Xing Gao, Weiyao Lin, Guo-Jun Qi, and Hongkai Xiong. 2020. Spatial-Temporal Transformer Networks for Traffic Flow Forecasting. arXiv:2001.02908 [eess.SP]
- [31] Masoud Yaghini, Mohammad M Khoshraftar, and Masoud Seyedabadi. 2013. Railway passenger train delay prediction via neural network model. *Journal of advanced transportation* 47, 3 (2013), 355–368.
- [32] Qi Zhang, Jianlong Chang, Gaofeng Meng, Shiming Xiang, and Chunhong Pan. 2020. Spatio-Temporal Graph Structure Learning for Traffic Forecasting. *Proceedings of the AAAI Conference on Artificial Intelligence* 34, 01 (Apr. 2020), 1177–1185. <https://doi.org/10.1609/aaai.v34i01.5470>

## A REPRODUCIBILITY

### A.1 Data preparation

Data cleaning is mentioned in Section 5, our preparation consists in removing duplicate observations that regularly occur in BREHAT data, and permuting observations in the wrong order. Duplicates can be detected thanks to an extra rank variable in BREHAT in BREHAT data: each RP along a train’s path is assigned a rank from 1 to the number of expected observations. These ranks are discontinuous, i.e. there are many ranks missing, and are not unique per observation: when a train arrives and departs from a train station, there are two distinct observations with the same rank but different observation types. We first re-order ranks when they are disordered, by using observation times to correct mistakes in said order. These errors are most often due to an imperfect circulation plan being used to create BREHAT data. We then filter all duplicate observation that have same rank, observation type, RP and train number for a given day.

### A.2 Data

The two following data is published alongside the paper [1]:

- Raw BREHAT data for the second week of 2018, containing all fields described in Subsection 3.2, as a set of JSON files,
- Training data generated from said data for the same week, using the process detailed in Subsection 4.1, as a set of JSON files.

The full dataset cannot be released for industrial competition reasons.